The function of mitogen activated protein kinases in zebrafish development

Krens, S.F.G.

IV

Distinct functions for ERK1 and ERK2 in cell migration processes during zebrafish gastrulation

S. F. Gabby Krens, Shuning He, Gerda E. M. Lamers, Annemarie H. Meijer, Jeroen Bakkers, Thomas Schmidt, Herman P. Spaink, B. Ewa Snaar-Jagalska

submitted

Abstract

The MAPKs are key regulatory signaling molecules in many cellular processes. Here we define differential functions for ERK1 and ERK2 MAPKs in zebrafish embryogenesis. Morpholino knockdown of ERK1 and ERK2 resulted in cell migration defects during gastrulation, which could be rescued by co-injection of the corresponding mRNA. *Erk2* mRNA cross-rescued ERK1 knockdown, but *erk1* mRNA was unable to compensate for ERK2 knockdown. Cell-tracing experiments in knockdown embryos revealed a convergence defect for ERK1 morphants without a severe posterior-extension defect, whereas ERK2 morphants showed a more severe reduction in anterior-posterior extension. These defects were primary changes in gastrulation cell movements and not caused by altered cell fate specification. More stringent knockdown conditions showed that the absence of dual-phosphorylated ERK2 from the blastula margin blocked initiation of epiboly and arrested embryogenesis, whereas ERK1 knockdown had only a mild effect on epiboly progression. Together, our data show distinct roles for ERK1 and ERK2 in developmental cell migration processes during zebrafish embryogenesis.

Introduction

The mitogen-activated protein kinase (MAPK) cascade governs key signaling pathways that control cell proliferation, differentiation and survival responses in all eukaryotes. Altered MAPK signaling is associated with developmental defects and various pathologies, including cancer. The MAPK cascade involves sequential activation of a serine/threonine kinase (MAPKKK), followed by a dual-specific MAPK kinase (MAPKK) and a dual-phosphorylated MAPK target. The vertebrate family of MAPKs consists of three major subfamilies: ERK, JNK and p38 (Johnson and Lapadat, 2002). An important challenge is to understand the complexity of the different MAPK cascades. Although specificity of these cascades has been reported (Kolch, 2005), it is clear that cross-talk occurs and strong indications for redundancies exist (Johnson et al., 2005). Distinct cellular functions in cancer formation have recently been shown for ERK1 and ERK2, which are the most intensively studied MAPKs of the ERK subfamily (Lloyd, 2006). For example, tumorigenicity of transplanted NIH 3T3 cells stably expressing an oncogenic form of Ras in nude mice was largely inhibited by co-transfection of ERK1, but not by ERK2 or p38 (Vantaggiato et al., 2006).

The canonical pathways of ERK1/2 activation are well studied *in vitro* and different animal models have been used to address ERK1 and ERK2 functions

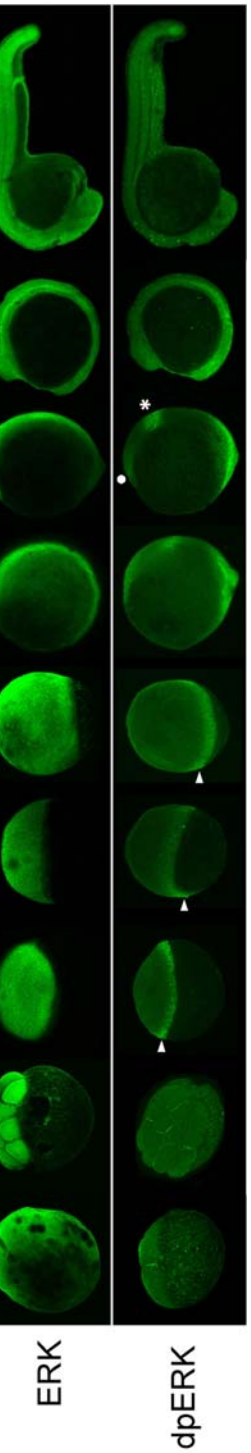

Figure 1. Spatio-temporal distribution of total ERK protein, compared to active dual-phosphorylated ERK (dpERK) protein by immuno-histochemistry. The dpERK signal was stronger on the cleavage-sites (2-cell and 16-cell stage). During gastrulation dpERK signal was enhanced in the margin (▲). After completion of gastrulation stronger signals were observed in the tailbud, MHB (*) and the anterior neural boundary (•). (5x objective, Biorad confocal laser scanning microscope)

in development. However, due to their crucial roles in early embryogenesis, the differential functions of ERK1 and ERK2 are not yet clearly defined. In *Drosophila*, FGF-dependent ERK activation was shown to be required for proper mesoderm dispersal (Gabay et al., 1997;Gryzik and Muller, 2004;Stathopoulos et al., 2004;Wilson et al., 2005) In chick, functions for activated ERK1/2 in axon growth were suggested (Kato et al., 2005). In *Xenopus*, ERK2 was shown to be required for mesoderm differentiation (Gotoh et al., 1995) and neural specification (Umbhauer et al., 1995;LaBonne et al., 1995;Uzgare et al., 1998). Studies using knockout mice clearly indicated that ERK1 and ERK2 have distinct functions. Gene disruption of *erk2* is lethal during early development, showing that ERK1 is not redundant to ERK2 (Yao et al., 2003). In contrast, *erk1*-/- mice are viable, fertile and of normal size. However, the proliferation and maturation of the thymocytes is affected, despite expression of ERK2 (Gilles Pagès et al., 1999) . Furthermore, ERK1 has a critical regulatory role in long-term adaptive changes of the brain, underlying striatum-dependent behavioral plasticity and drug addiction (Mazzucchelli et al., 2002). *Erk1*-/- mice showed improved rate of learning and better long term memory than wild type controls. Elevated ERK2 activation was observed in primary neurons isolated from *erk1* knockout mice, whereas no higher ERK2 levels were detected in the brains. Mouse embryos lacking exon 2 of the *erk2* gene die *in utero* before embryonic day (E) 8.5 due to a defect in trophoblast development. *Erk2*-deficient mice fail to form the ectoplacental cone and the extra-embryonic ectoderm, which gives rise to mature trophoblasts in the fetus (Saba-El-Leil et al., 2003). *Erk2*-/- embryos also fail to form mesoderm, based on histological criteria at E6.5 and E7.5 (Yao et al., 2003). Finally, ERK2 is critical for proliferation of the trophoblast stem cell-population present in the trophectoderm and proximal extra-embryonic ectoderm, which is essential for placenta formation (Ornitz and Itoh, 2001).

In this study we aimed to increase the understanding of the differential roles of ERK1 and ERK2 in early vertebrate embryogenesis and cell-migration processes, using the zebrafish model. Because of its *ex utero* development the zebrafish model is optimally suitable to study the link between the cellular and developmental functions of ERK1 and ERK2. Previously, immunohistochemical analysis of the spatio-temporal patterns of ERK1/2 phosphorylation showed that, like in mouse (Corson et al., 2003) and chick (Delfini et al., 2005), zebrafish ERK1/2 is activated locally during segmentation stages (Sawada et al., 2001). Furthermore, it was shown that insulin-like growth factors (IGFs) stimulated zebrafish cell proliferation by activating ERK-MAPK and PI3-kinase signaling pathways (Pozios et al., 2001). Subsequently, research on the ERK-MAPK pathway in zebrafish development has mostly concentrated on the functions of the FGF/MAPK pathway, which also contains the

inhibitors Sef (Furthauer et al., 2002;Tsang et al., 2002) , Sprouty2/4 and the MAPK phosphatases MKP1 and MKP3 (Tsang et al., 2004). Over-activation of the FGF/ERK-pathway led to dorsalized embryos by inhibiting expression of BMP genes (Furthauer et al., 2004). In contrast, over-expression of ERK-MAPK phosphatase MKP3 or injection of a high dose of mRNA of the inhibitor *Sef* resulted in an opposite ventralization (Furthauer et al., 2002;Tsang et al., 2004). More recently, endoderm formation was shown to be regulated by combinatorial Nodal, FGF and BMP signaling, where BMP and FGF signaling cooperate to endoderm formation in response to Nodal signaling (Poulain et al., 2006). Recently, we identified the zebrafish orthologs of the MAPK gene family and determined their specific spatial and temporal expression patterns during zebrafish embryogenesis (Krens et al., 2006). We showed that the zebrafish genome encodes for members of all MAPK-subfamilies; ERK, JNK and p38. Furthermore, we showed that *erk1* and *erk2* are differentially expressed compared to each other and to the other members of the zebrafish MAPK gene-family. However, no gene-targeting studies have been reported until now.

Here, we report on knockdown studies of ERK1 versus ERK2 and present evidence for differential effects on convergence extension cell movements. Cell tracing experiments showed that ERK1 morphants displayed reduced convergence cell movements, whereas ERK2 morphants showed a more severe reduction in anterior-posterior extension of the dorsal body axis, without significantly altering the early cell fate specification. Stronger knockdown conditions for ERK2 arrested embryogenesis at the onset of epiboly, thereby preventing the blastula to gastrula transition. Taken together, our data imply distinct functions for ERK1 and ERK2 MAPKs in gastrulation cell migration during zebrafish embryogenesis

Results and discussion

Immuno-histochemical analysis of the localization of active / phosphorylated ERK1 and ERK2 MAPK showed elevated levels of ERK phosphorylation in the cleavage furrows at the 16 cell stage, in the margin during epiboly and gastrulation, at locations of neural differentiation (anterior neural boundary and mid-hindbrain boundary, Fig.1) and segmentation (Pozios et al., 2001;Sawada et al., 2001). Immunohistochemistry cannot distinguish between ERK1 and ERK2. However, we recently showed that *erk1* and *erk2* display differential spatiotemporal expression patterns during zebrafish development (Krens et al., 2006), suggesting distinct functions for ERK1 and ERK2 during zebrafish development.

Morpholino knockdown of ERK1 and ERK2 results in specific phenotypes

To elucidate the functions of ERK1 and ERK2 in zebrafish development, gene-specific morpholinos (MO) directed to the 5' untranslated sequences were used to block the translation of *erk1* or *erk2* mRNAs. Injection of 0.2mM (1.7 ng) ERK1MO or ERK2MO induced severe developmental defects (Fig.2), while treatment with the same concentration of the standard control MO had no effect (data not shown). At 24 hpf approximately 10% of ERK1MO injected embryos were dead, and 85% (n=130) displayed phenotypes characterized by a shorter body axis and somites without the distinct v-shape (Fig.2A). The somitogenesis phenotype was confirmed by in situ hybridization with *myod* (supplemental data Fig.S1). In contrast, ERK2MO injected embryos (n=75) showed approximately 70% lethality at 24 hpf and 85% at 48 hpf (Fig.2E) and the surviving ERK2MO morphants showed more severe phenotypes than the ERK1 morphants. At 24 hpf, the head was still distinguishable, but the MHB was not properly formed as shown by lack of *pax2.1* gene expression (Brand et al., 1996). In addition, development of the tail structures was severely defected (Fig.2B, Fig.S1), resulting in shortened phenotypes at 48 hpf (Fig.2G). Somites structures were barely recognizable and the associated *myod* expression pattern was highly aberrant (Fig.S1). Approximately 50% of the embryos treated with ERK1MO and 15% treated with ERK2MO survived up to 48 hpf (Fig.2E). The surviving morphants were shortened at 24 and 48 hpf and had enlarged heart-cavities (Fig.2F,G). Protein analysis of the surviving embryos by western blot using a general ERK antibody showed that ERK1 and ERK2 protein levels were specifically and significantly reduced by the respective ERK1 and ERK2 MOs (Fig.2D).

To test the specificity of the obtained knockdown phenotypes, rescue experiments were performed using synthetic *erk1* and *erk2* mRNAs lacking the MO target site. Protein samples were made at the shield stage from embryos injected with 100 pg mRNA and western blot analyses showed that the synthetic mRNAs were correctly translated into proteins and were dual phosphorylated/activated in the embryo (Fig.S2B). For rescue experiments mRNA concentrations were used below those that induced over-expression phenotypes (Fig.S2). Co-injection of synthetic *erk1* mRNA (8 pg per embryo) with 0.2 mM ERK1MO rescued 67% of embryos with the shorter body axis at 24 hpf and 50% at 48 hpf (Fig.2E,F,H,J and L). Co-injection of *erk2* mRNA (1.5 pg per embryo) with 0.2 mM ERK2MO increased the percentage of survivors from ~20% to more than 70% at 24hpf and rescued the body axis defect in ~35% of the embryos (Fig.2E, G-M). The redundancy of the ERK1 and ERK2 was determined in cross-rescue experiments using the same mRNA concentrations as described above (Fig.2E and data not shown). ERK1 knockdowns were

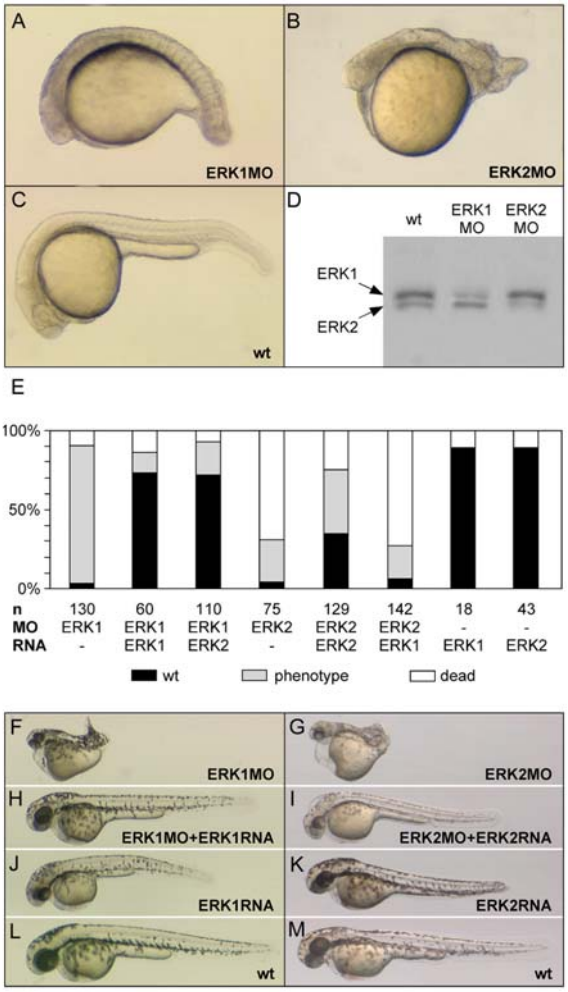

Figure 2. Specific ERK1 and ERK2 knockdown by morpholino injection. (A-C) Images show representative examples of the ERK1 (A) or ERK2 (B) knockdown phenotypes at 24 hpf, compared to wild type (wt) embryos (C). Specific knockdown was confirmed by Western blot analysis optimized to discriminate between the sizes of ERK1 (p44MAPK) and ERK2 (p42MAPK) protein and detected with global ERK antibody (D). Protein samples were isolated from 20 hpf embryos, injected with 0.2mM ERK1-MO or ERK2-MO. (E) Statistics of ERK knockdown and (cross-) rescue experiments determined by co-injection of ERK1 or ERK2 morpholino with synthetic *erk1* or *erk2* mRNA at 24 hpf. Black = wild type; gray = phenotype; white = dead.
(F-M) Images show phenotypes of surviving knockdown embryos at 48 hpf (F,G), embryos rescued by co-injection of corresponding mRNA (8pg *erk1* RNA, 1.5pg *erk2* RNA) (H,I), embryos injected with mRNA only (J,K) and wild type embryos at 48hpf (L,M)

rescued by co-injection of *erk2* mRNA with similar efficacy as by *erk1* mRNA. Co-injection of ERK2MO with *erk1* mRNA did not increase the number of surviving embryos nor rescued the body axis defects, indicating that the amount of *erk1* mRNA that rescued ERK1 knockdown cannot cross rescue the ERK2 knockdown phenotype.

Distinct functions for ERK1 and ERK2 in gastrulation cell movements

The low surviving rates and the severe phenotypes of ERK1 and ERK2 morphants at 24hpf indicate possible roles for these kinases in earlier developmental processes. To address this, embryos injected with ERK1MO or ERK2MO were closely monitored at yolk plug closure (YPC) until tailbud stages (Fig.3A-F). ERK1MO-injected embryos showed rather normal extension compared to control embryos (Fig.3A,B, distance between arrowheads), but showed a widening of the dorsal axial mesoderm structures (notochord, Fig.3D,E). Strikingly, ERK2MO-injected embryos showed a shortened anterior-posterior axis at the end of gastrulation (Fig.3C), but a far less severe effect on the widening of the notochord than ERK1MO-injected embryos (Fig.3F).

These results pointed towards a possible effect of ERK1 and ERK2 knockdown on dorsal-ventral patterning or convergence extension (CE) cell movements. We first addressed this question, using the marker genes *dlx3*, expressed in the neural plate, *sonic hedgehog* (*shh*), expressed in the notochord, and *hgg1*, expressed in the developing hatching gland, in 10 hpf embryos (Fig.3G-L) as previously described (Jopling and den Hertog, 2005). In ERK1 morphants, the *dlx3*-expression domain was much wider and the hatching gland was located more posterior (Fig.3H,K). Strikingly, ERK2 morphants did not show this widening of the neural plate (*dlx3*), suggesting that this defect was ERK1MO specific. In ERK2 morphants (Fig.3I,L) the *sonic hedgehog* (*shh*) expression domain in the midline was not fully extended in the anterior direction, resulting in a gap between the *dlx3* and shh expression domains. In addition, the expression domain of *hgg1* was located even more posterior than in ERK1 morphants, indicating affected extension in ERK2 morphants.

Depletion of ERK1 or ERK2 perturbs gastrulation cell movements differently, without significantly altering early cell fate specification

In order to address if the observed phenotypes in ERK1 and ERK2 knock down embryos were primary cell movement defects or secondary effects due to a patterning alteration we performed in situ hybridization with several different marker genes (Fig.4).

In ERK1MO injected embryos at late gastrula stages, in situ hybridization for markers of dorsal ventral patterning revealed a slight reduction of the ventral non neural ectoderm marker gene *gata2* (Fig.4B) and a concomitant expansion of the dorsal neural ectoderm marker *otx2*, suggesting mild dorsalization of ERK1MO embryos (Fig.4E). The expression domain of *cyclops* in the *axial* mesoderm was mediolaterally expanded (Fig.4H). This observation was confirmed with the non-axial mesoderm marker *snail1a* (Fig.4K) showing a bigger

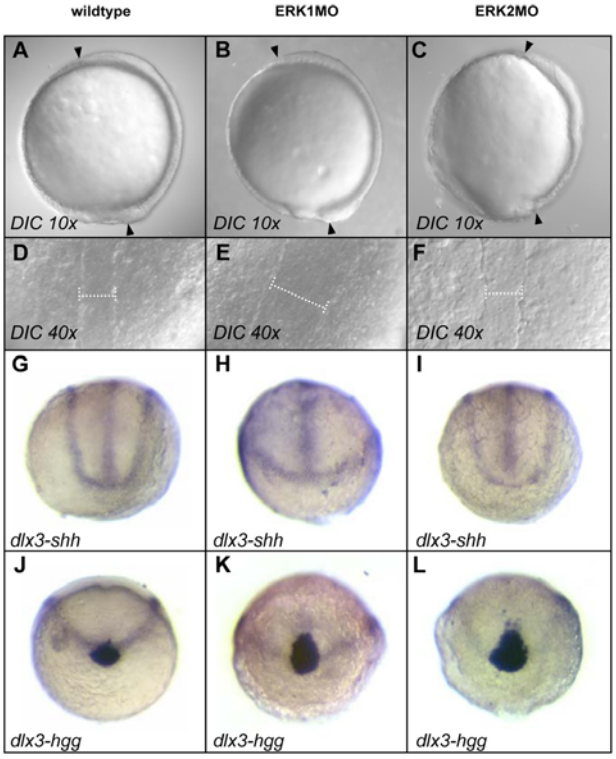

Figure 3. Phenotypic characterization of ERK1 and ERK2 morphants in late- gastrulation and early segmentation indicates affected convergence extension movements. (A,D,G,J); wild type control embryos (B,E,H,K); ERK1 knockdown embryos, injected with 1.7ng ERK1MO (C,F,I,L); ERK2 knockdown embryos, injected with 1.7ng ERK2MO. (A-C); Live embryos at yolk plug closure (YPC) to tailbud (TB) stages, animal pole up, dorsal to right. The distance between the arrowheads (►) resembles the length of the AP body axis (10x objective), or dorsal view (D-F), white spacer highlights the widening of the dorsal notochord (40x objective). (G-L); Combined in situ hybridization on 10 hpf old embryos with *dlx3* (edge neural plate), with *shh* (midline) or with *hgg1* (hatching gland) marker-genes (anterior view, dorsal to top).

gap in its expression at the dorsal axis and a broadening forerunner cells as detected by the endoderm marker gene *sox17* (Fig.4N). These changes were not observed in ERK2 knockdowns (Fig.4C,F,I,L and O)

In ERK2 morphants the expression domains of *gata2* and *otx2* were reduced (Fig.4R and U) as *gata2* and *otx2* expression did not expand as far ventrally and dorsally respectively compared to wild type and ERK1MO embryos (Fig.4P,S and Q,T). Analogous, the expression domain of *cyclops* and *notail* was shortened in the anterior-posterior axis in ERK2MO injected embryos (Fig.4X,A'), compared to wild type embryos (Fig.4V,Y) and ERK1 morphants (Fig.4W,Z). Consistent with the normal fate specification and regionalization in both ERK1MO and ERK2MO embryos at later gastrulation stages, normal expression of earlier patterning marker genes was observed. The dorsalizing factor *chordin* was expressed normally at 30% epiboly (Fig.4B'-D'), as was *goosecoid*, expressed at the dorsal margin (Fig.4E'-G'). Taken together, the expression patterns of different cell fate marker-genes indicated some slight morphological changes specific for either ERK1MO or ERK2MO, but the global cell patterning was not changed in these morphants. Therefore, these results suggest that ERK1 and ERK2 knockdown perturb gastrulation by affecting cell movements, without significantly altering the early cell fate specification.

In order to directly study the specific effect of ERK1 and ERK2 knockdown on cell movements during gastrulation, we performed cell-tracing experiments using DMNB-caged fluorescent dextran (Kozlowski et al., 1997;Sepich et al., 2000). To follow convergence (dorsal) cell migration, lateral mesoderm cells located 90° from the dorsal shield, were labeled by uncaging the fluorophore with a localized pulse of ultraviolet light at 6hpf and followed in time (Fig.5A-I and S). Extension cell migration processes were monitored by labeling cells in the dorsal shield (Fig.5J-R and T).

ERK1MO-injected embryos displayed a severely reduced movement of the labeled lateral cells towards the dorsal axis in time (Fig.5A-C), whereas only a slight reduction of dorsal migration was observed in ERK2MO-injected embryos (Fig.5D-F). In contrast, in ERK2MO injected embryos the extension movements were reduced to a greater extend, compared to ERK1MO injcted embryos that showed rather normal extension movements. Quantification of 10 embryos indicated that the reduction of dorsal migration for ERK1 (Fig.5S) and the reduced anterior extension migration for ERK2 (Fig.5T) were significant, and confirm the previous suggestions based on the in situ hybridization results (Fig.3 and 4). Together, these results indicate differential affected CE movements by ERK1 or ERK2 knockdown.

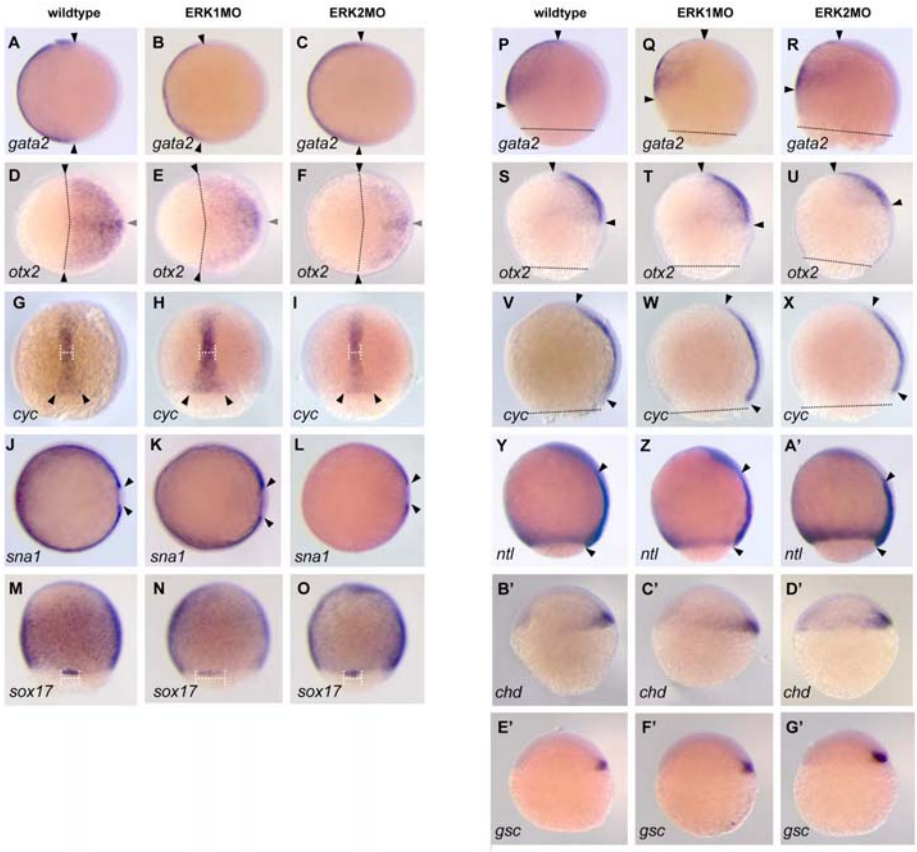

Figure 4. Expression of embryonic patterning marker genes in ERK1 and ERK2 morphants
Expression of mRNA was detected by whole mount in situ hybridization. (A-F, J-L) animal pole view, dorsal to right; (G-I,M-O) dorsal view, animal pole to top; (P-G') lateral view, dorsal to right, animal pole to top.
(A-C, P-R) *gata2*, expressed in non-neural ectoderm at 80% epiboly.
(D-F, S-U) *otx2*, expressed in ectoderm at 90% epiboly.
(G-I, V-X) *cyclops*/*ndr2* in axial mesoderm at 80-90% epiboly.
(J-L) *snail1a* in paraxial mesoderm at 90% epiboly.
(M-O) *sox17* in endoderm and forerunner cells at 80% epiboly.
(Y-A') *notail* in margin an axial mesoderm at 90% epiboly.
(B'-D') *chordin* in presumptive dorsal shield.
(E'-G') *goosecoid* in presumptive dorsal shield.

Arrowheads (►) mark the boundaries of expression domains.

ERK1 knockdown mildly affects epiboly progression, whereas ERK2 knockdown causes a developmental arrest at the onset of epiboly

Taken into account that the knockdown of ERK1 and ERK2 was not completely saturated (Fig.2D), we applied more stringent knockdown conditions by doubling the MO concentration and studied the effects on epiboly (Fig.6 and S3). Embryos injected with 0.2 mM ERK1MO (Fig.S3A) did not show any obvious phenotype until 80% epiboly, while doubling the concentration to 0.4 mM slightly delayed epiboly-migration compared to wild type embryos (Fig.S3B). Embryos injected with 0.2 mM ERK2MO were delayed to 65% epiboly at 8hpf (Fig.S3C), when wild type embryos reached 80%. Knockdown of ERK2 by injection of 0.4 mM ERK2MO prevented epiboly cell in 38% (Fig.6-arrest category and Fig.S3D) of the injected embryos and inhibited epiboly progression and further progression into gastrulation stages in 46% of the embryos (Fig.6 severe). This effect was rescued by co-injection of 20 pg synthetic *erk2* mRNA (Fig.S3E), which resulted in 82% (49 out of 60 embryos) of the co-injected embryos entering gastrulation. Injection of this amount of synthetic *erk2* mRNA did not induce any phenotype by itself at this stage.

Nomarski microscopy was performed to study the affected epiboly initiation at 4.5hpf (Fig.7A-F). The leading edge of the migrating cells in the margin and the enveloping layer (EVL) in wild type embryos (Fig.7A,D) and ERK1MO embryos (Fig.7B,E) showed a sharp front of migrating cells over the yolk. Knockdown of ERK2 induced a discontinuity in the margin and delayed crowding of the yolk syncytial nuclei (YSN) in the external yolk syncytial layer (YSL), resulting into a broadened YSL (Fig.7C, F).

Taking into account that active/phosphorylated ERKs were previously detected in the margin (Fig.1), we performed immuno-histochemistry against the dual phosphorylated ERK1/2 at 4.5hpf (dome-30% epiboly) and 8hpf (80% epiboly) (Fig.7G-I and J-L). In the control embryos (G,J) and the ERK1MO injected embryos (H,K) phosphorylated ERK was still detected in the margin in both stages. However, ERK phosphorylation was completely abolished in ERK2MO injected embryos (I,L) at both stages, indicating that ERK2 is the active ERK MAPK in the margin during gastrulation cell moments and that ERK2 plays a key-role in epiboly progression.

The migration of the YSN to the vegetal pole is considered as a driving force, next to radial intercalation (Myers et al., 2002; Montero and Heisenberg, 2004; Solnica-Krezel, 2006), through all stages of epiboly (Kane et al., 1996). At late blastula stages, the YSL forms a broad band and contains most of the YSN. At sphere/dome stage, the wide belt of external YSL narrows in the animal-vegetal direction and the YSN become increasingly crowded. When the blastoderm expands vegetally reaching 30% epiboly, the YSN of the exter-

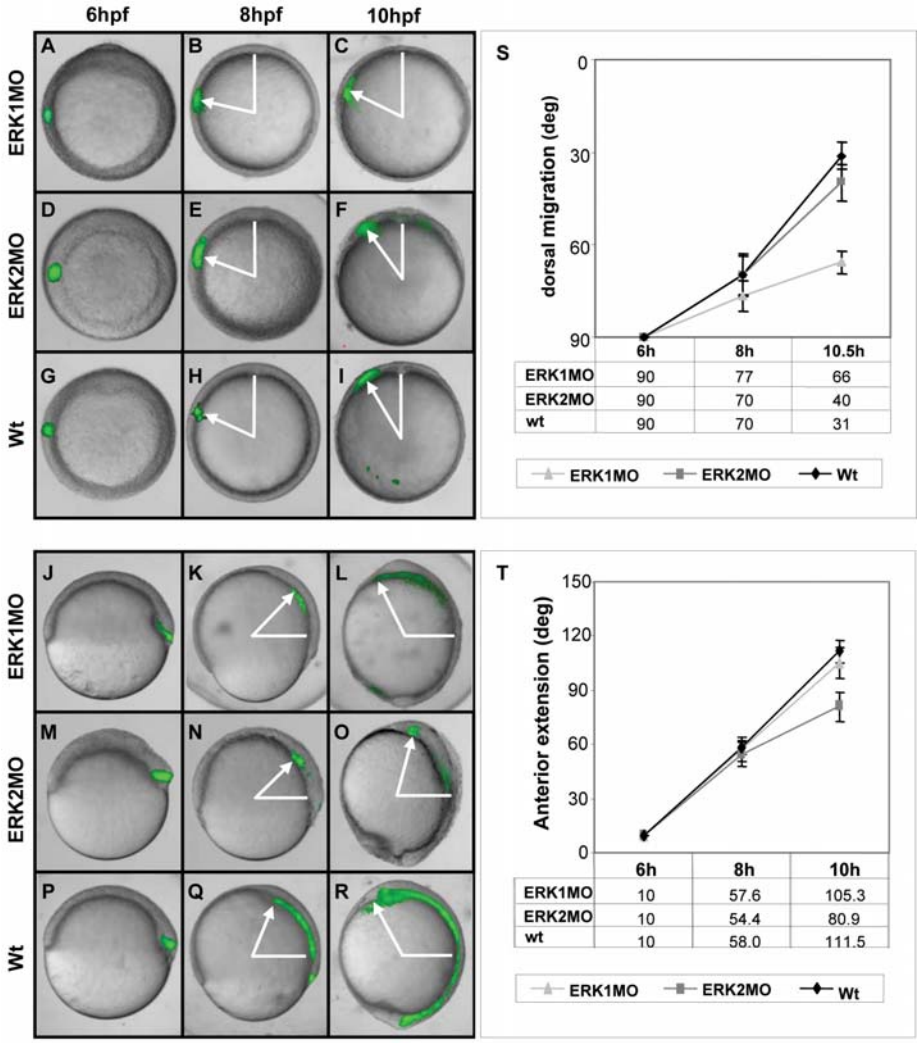

Figure 5. Knockdown of ERK1 and ERK2 affects CE cell movements differentially. Embryos were co-injected with MO and caged fluorescein dextran, which was activated at shield stage (6hpf) laterally to determine dorsal migration (A-I; animal pole view, dorsal to top) and dorsally to determine anterior extension (J-R; lateral view, dorsal to right). Images show uncaging cells directly after activation (A,D,G,J,M,P), at 8hpf (B,E,H,K,N,Q) and at 10hpf (C,F,I,L,O,R). Cell tracing experiments were performed in ERK1MO injected (A-C, J-L), ERK2MO injected (D-F, M-O) and wild type embryos (G-I, P-R). (S) Quantification of dorsal migration (n=10 embryos), measured as indicated with white arrows (A-I) as degrees from dorsal. (T) Quantification of anterior migration measured as indicated with white arrows (J-R) as degrees of anterior movement (n=10 embryos). ERK1MO: gray triangle, ERK2MO: dark gray square, wild type: black diamond.

nal YSL concentrate near the EVL at the margin (Solnica-Krezel and Driever, 1994). To follow migration of the YSN *in vivo,* 10 µM SYTOX-green nucleic acid stain was (co-)injected in wild type control embryos and morpholino-treated embryos (Fig.7M-O). At 8 hpf, ERK1 knockdown resulted in a delay of epiboly movements. Control embryos were at 80% epiboly (Fig.7M) when ERK1MO injected embryos were still at 50% epiboly (Fig.7N). In ERK2 morphants the YSN were still located at the top of the yolk at 8hpf and did not show any migration towards the vegetal pole (Fig.7O). Therefore we conclude that knockdown of ERK2, and subsequent depletion of activated ERK2 from the margin, also prevented the YSL from migrating to the vegetal pole of the embryo.

Together, these results provide evidence that knockdown of ERK1 and ERK2 affects convergence extension cell movements differentially during zebrafish gastrulation, without significantly altering early developmental patterning. ERK1 morphants showed a reduced convergence defect without a severe anterior posterior extension defect, whereas ERK2 morphants did show a severe anterior posterior extension defect without a significant convergence defect. Further analysis, using stronger knockdown conditions revealed that ERK2 is the active MAPK in the blastula margin. This indicates that absence of this active ERK2 from the margin at the blastula to gastrula transition prevents the initiation of epiboly. This subsequently blocks further progression of gastrulation cell migration processes, leading to an arrest in embryogenesis.

Discussion

The ERK1 and ERK2 MAPKs are among the most studied signaling molecules and numerous important functions for these proteins in cellular and developmental signaling processes have been observed. However, the specificity of MAPKs in developmental processes is not well understood. In this study, we show that ERK1 and ERK2 have distinct roles in epiboly and convergence extension (CE) movements. Specifically, we present data demonstrating that ERK1 knockdown affects convergence to a larger extend, whilst ERK2 knockdown predominantly affects anterior-posterior extension during gastrulation cell migration processes. In addition, complete depletion of active ERK2 from the blastula margin prohibited epiboly initiation and led to an arrest of embryogenesis.

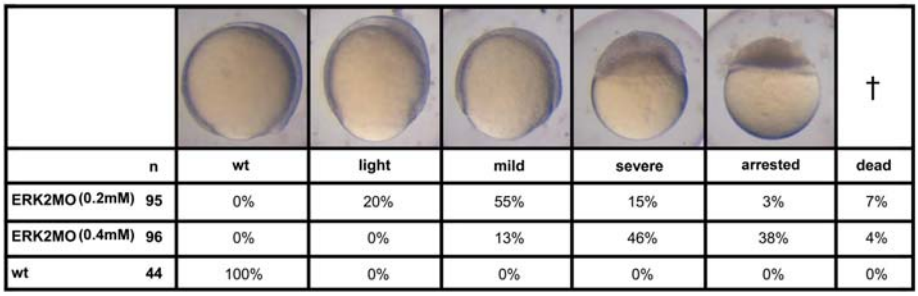

	n	wt	light	mild	severe	arrested	dead
ERK2MO (0.2mM)	95	0%	20%	55%	15%	3%	7%
ERK2MO (0.4mM)	96	0%	0%	13%	46%	38%	4%
wt	44	100%	0%	0%	0%	0%	0%

Figure 6. Classification of the phenotypes of embryos injected with 0.2 mM or 0.4 mM ERK2MO, compared to wild type embryos at 8-9 hpf. Classification into wild type, light, mild, severe and arrested phenotype categories is indicated by percentages.

Different lethality of ERK1 versus ERK2 knockdown

Morpholino knockdown of ERK1 and ERK2 resulted in a shorter body axis and affected somite shape. Knockdown of ERK2 also disrupted the formation of the MHB and was more lethal than knockdown of ERK1 (Fig.2 and S1). Similar phenotypes were observed in previous studies after inhibition of the FGF pathway with the FGFR inhibitor SU5402, by over-expression of a dominant negative FGF receptor, and in embryos lacking FGF8 and FGF24 ligand activity (Griffin et al., 1995;Draper et al., 2003;Griffin and Kimelman, 2003;Mathieu et al., 2004), suggesting that the functions of ERK1 and ERK2 are linked to FGF signaling in zebrafish.

The observation that ERK2 knockdown is more lethal than ERK1 knockdown is in agreement with gene targeting results in mice showing that *erk1*-/- mice are viable and without embryonic phenotypes, whereas *erk2*-/- mice are lethal (Gilles Pagès et al., 1999). In zebrafish, the same amount of *erk2* mRNA that rescued morpholino knockdown of ERK2 was also able to cross-rescue knockdown of ERK1. In contrast, the *erk1* mRNA could not cross-rescue ERK2 morphants. Our results support the suggestion of Yao et al. that ERK2 can compensate for the loss of ERK1 (Yao et al., 2003;Saba-El-Leil et al., 2003). The difference between the observed developmental defects and lethality in zebrafish ERK1 morphants and the lack of a severe phenotype in *erk1*-/- mice (Mazzucchelli et al., 2002) is remarkable and suggests different redundancy and adaptation mechanisms in these organisms.

Distinct roles for ERK1 and ERK2 in convergence and extension cell movements during gastrulation

Phenotypes of surviving ERK1 and ERK2 morphants indicated possible effects on the dorsal-ventral patterning and convergence extension cell movements. In situ hybridization using combinations of markers for these processes supported this hypothesis (Fig.3), while in situ hybridization experiments with patterning marker genes did not show a significant altering of the early cell fate specification (Fig.4). The expression domain of *dlx3*, as a marker for the edge of the neural plate, was widened in ERK1 morphants and in ERK2 morphants a gap was observed between the expression-domains of *dlx3* and *shh* (notochord). This showed a distinct loss-of-function defect of ERK1 versus ERK2 during gastrulation cell migration processes. In order to directly define the specific functions of ERK1 and ERK2 in convergence extension (CE) cell movements, cell tracing experiment were performed in ERK1 and ERK2 morphants (Fig.5). We found distinct defects upon ERK1 and ERK2 knockdown during CE movements, as ERK1 morphants showed a convergence defect without a severe posterior-extension defect, whereas ERK2 morphants showed a more severe reduction in anterior-posterior extension. Importantly, defects underlying CE movements were primary effects, and not secondary to patterning defects, since in situ hybridization analyses with marker genes revealed no significant patterning changes in ERK1 and ERK2 morphants (Fig.4).

The CE movements during zebrafish gastrulation involve different cellular events, depending on the position of the cells along the dorsoventral axis (Myers et al., 2002). Dorsal convergence appears to require migration of cells on the extracellular matrix, while extension movements might be more dependent on cell-cell adhesion, involving neighboring cells crawling over the surfaces of the surrounding cells. Importantly, these findings are consistent with recent zebrafish work demonstrating that convergence and extension cell movements may be considered as separate morphogenetic movements of gastrulation cell migration in zebrafish (Glickman et al., 2003;Bakkers et al., 2004;Daggett et al., 2004).

In other model systems interaction between ERK signaling and cell migration during gastrulation were also observed. In *Drosophila*, *Xenopus*, mouse and zebrafish, the functions of ERK MAPKs are related to FGF signaling. Throughout zebrafish development, activated ERK protein is localized in overlapping expression regions with various FGF ligands and other components of the FGF-pathway (Fig.1) (Pozios et al., 2001;Sawada et al., 2001;Furthauer et al., 2002;Tsang et al., 2002;Poulain et al., 2006). In the early mouse gastrula, FGFs are required for the migration of the epiblast cells out of the primitive streak, which consists of the endoderm and mesoderm progenitor cells (Sun

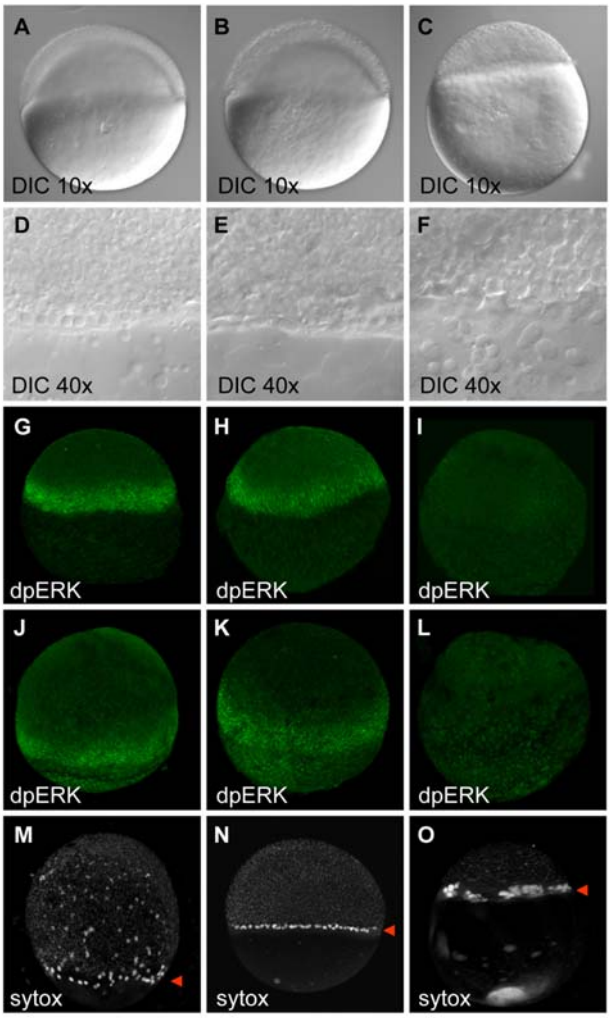

Figure 7. Stronger knockdown of ERK2 prohibits epiboly initiation and revealed ERK2 to be the active MAPK in the margin. Embryos were injected with 0.4mM (3.4 ng) ERK1MO or ERK2MO and compared to wild type embryos at the indicated stages. Differential interference contrast (DIC) microscopy using a 10x objective (A,B,C,) or a 40x objective (D,E,F) was used to monitor the onset of gastrulation (4.5hpf). Localization of dpERK was detected by immuno-localization in wild type, ERK1MO and ERK2MO injected embryos at 4.5 hpf (G-H) and 8hpf (J-L) by phospho-specific ERK antibody. YSL-migration was followed by co-injection of 10µM sytox green, red arrowhead, 8hpf (M,N,O). Images in G-O were taken by confocal microscopy.

et al., 1999). In chicken, FGFs signal chemotactic cues during gastrulation, and coordinate cell movements during ingression of the epiblast cells through the primitive streak (Yang et al., 2002). During early mesoderm migration in *Drosophila*, the local MAPK activation pattern suggests that the FGF receptor (Htl) is specifically activated at the leading-edge of the migrating mesoderm cells (Gabay et al., 1997), with FGF8-like1 and FGF8- like2 being required as ligands for Htl (Gryzik et al., 2004). Here we showed that disruption of these signals by knockdown of either of the key FGF downstream targets ERK1 or ERK2 results in differential effects on the regulation of convergence extension movements. This also points towards different downstream targets of ERK1 and ERK2 and divergence of ERK-signaling at this level.

Epiboly initiation requires active/phosphorylated ERK2 in the blastula margin

More stringent knockdown conditions were applied to address the possible functions of ERK1 and ERK2 as phosphorylated ERK1 and ERK2 were previously detected in the blastula margin (Fig.1). The increased knockdown of ERK1 only slightly delayed epiboly, whereas 40% of the ERK2MO injected embryos did not initiate epiboly at all. Immuno-histochemical studies on ERK1 and ERK2 morphants using a phospho-ERK antibody showed that ERK2 is specifically activated in the blastula margin (Fig.7I and L) and crucial for epiboly progression. Our results indicate that depletion of this active ERK2 from the margin prevents cells from the animal pole to migrate over the yolk-cell at the onset of epiboly (Fig.7). In addition, migration of the YSL to the vegetal pole was prevented, thereby removing one of the motors for gastrulation movements (Solnica-Krezel et al., 1994; D'Amico and Cooper, 2001; Solnica-Krezel, 2006).

Integration of ERK MAPKs in other developmental signaling networks

Our results suggest that activation of ERK2 plays a major role in early epiboly initiation. The question remains which signaling cascade. that triggers the onset of epiboly, is blocked by ERK2 knockdown. At the upstream signaling level multiple interconnected signaling pathways, such as Nodal, Wnt, BMP and FGF, act together to coordinate epiboly and gastrulation processes (Schier and Talbot, 2005) and are therefore possibly connected with ERK2 activation.

Similarities were observed between the severe phenotypes of ERK morphants and embryos in which the FGF pathway was inhibited. Mesoderm initiation was previously shown not to be affected in the absence of FGF signaling (Raible and Brand, 2001; Draper et al., 2003; Furthauer et al., 2004; Tsang

et al., 2004) as in severe ERK2 morphants that still expressed *ntl* and *papc* (data not shown). However, *erk2*-/- mice fail to form mesoderm (Yao et al., 2003). Attempts to block FGF signaling by triple knockdown of FGF8,17b and 24 did also not inhibit epiboly and endoderm/ectoderm differentiation as in ERK2 morphants, but resulted in a large increase of endoderm precursor cells (Poulain et al., 2006). This indicates that multiple pathways may be involved in the regulation of ERK2 in the margin at the onset of epiboly.

A number of mutants described for epiboly arrest show delayed or arrested epiboly at later stages, but not a block at blastula to gastrula transition (Kane et al., 1996). For example, different *hab* alleles, containing mutations in the cell adhesion molecule *E-cadherin* (*cdh1*), arrest epiboly of deep cells at mid-gastrulation, whereas epiboly of EVL and YSL proceeds further (Kane et al., 2005;Shimizu et al., 2005). Reduction of E-cadherin protein levels by morpholino knockdown also delayed epiboly and affected intercalation and possibly extension cell migration (Kane et al., 2005). Stronger loss of E-cadherin function impaired epiboly at earlier stages (Babb and Marrs, 2004), similar as observed in our study of ERK2 morphants. An interesting link is starting to emerge between activation of ERK MAPKs via hepatocyte growth factors and the regulation of *E-cadherin* expression via *snail* in cancer processes (Medici et al., 2006;Grotegut et al., 2006). In future studies we would like to address the link of ERK MAPK with FGF, E-cadherin and other signaling components using microarray analyses in the different ERK knockdown backgrounds.

Experimental procedures

Cloning

Total RNA was isolated from adult Tuebingen zebrafish, using TRIZOL® Reagent protocol (GIBCO BRL, Life technologies ™). cDNA for zebrafish *erk1* and *erk2* genes were cloned into pCR®4Blunt-TOPO® (Invitrogen) using primers flanking the coding region, based on EST AB030902 and AB030903, and subcloned in the pCS2+ vector using the EcoR1-site. Constructs were checked by sequence analysis.

Micro-injection of morpholinos and mRNAs

One-cell stage embryos were injected with 1 nl of the solubilized compounds in 1× Danieau's buffer [58 mM NaCl, 0.7 mM KCl, 0.4 mM $MgSO_4$, 0.6 mM $Ca(NO_3)_2$, 5.0 mM HEPES; pH 7.6] containing 1% Phenol red solution (Sigma). Definition of stages was according to Kimmel et al. At the 1K-stage (3hpf), embryos with a red animal pole were selected as positive-injected embryos. To block translation of the *erk1* or *erk2* mRNA, 1.7 ng or 3.4 ng of MOs were injected per embryo. MOs were targeted against the 5'- UTR of the respective mRNAs (GeneTools Philomath, OR, USA): ERK1MO, 5'-TCTGTCCGCAAATCGTCGCCTTCGC; ERK2MO, 5'-CACCCAAAAGCACCAGGAAAAGCTC.

The pCS2+ constructs containing the zebrafish ERK1 and ERK2 genes were linearized and synthetic mRNAs were transcribed with SP6 RNA polymerase using the mMessage mMachine Kit (Ambion). Per embryo 1 to 150 pg mRNA was injected.

Cell tracing

Embryos were (co-)injected at the one cell stage with 0.3% 4,5-dimethoxy-2-nitrobynzyl (DMND)-caged fluorescein dextran (molecular mass 10,000; Molecular probes, kind gift from the Hammerschmidt lab.). Uncaging was performed as previously described (Bakkers et al., 2004) with UV light at shield stage (6hpf) using a Zeiss axioplan microscope with 40x objective and adjustable pinhole. Embryos were imaged at 6, 8 and 10.5 hpf. The dorsal convergence and anterior extension angles were measured using Image J (NIH imaging software).

Whole-mount immuno-staining

Embryos were fixed overnight in 4% paraformaldehyde at 4°C. Embryos were washed three times and incubated for 2 hours in blocking buffer (PBS, 0.1% BSAc, 1% Triton X100) followed by overnight incubation at 4°C in 1:100 dilution of primary antibody (Polyclonal phospho-p44/42 MAP kinase antibody from Cell Signaling; ERK antibody K-23, Santa Cruz Biotechnology) in blocking buffer. Embryos were washed three times with blocking buffer, followed by 1 hour, incubation in 1:100 diluted secondary antibody (Goat anti-rabbit Alexa 488 conjugated). Embryos were washed three times in blocking buffer, and three times in PBS containing 0.1 % Tween.

Whole-mount in situ hybridization

Embryos were fixed overnight in 4% paraformaldehyde in PBS at 4 °C and in situ hybridization was performed as described previously (Thisse et al., 1993) using described probes for *chd*, *cyc*, *gsc*, *gata2 myod*, *ntl*, *otx2*, *pax2*.1, *snai1a*, *shh1*, *sox17*. The *dlx3* and *hgg1* probes were kindly provided by Jeroen den Hertog.

Protein isolation and western blot analysis

Embryos were dechorionated and de-yolked in Ca^{2+}/Mg^{2+} free solution. Cells were pelleted and washed with PBS followed by a passive lysis in buffer (0.125% NP40, 25mM Tris-HCl, 2 mM EDTA, 1 mM Na_3VO_4, 25 mM NaF and 1 complete mini EDTA-free protease inhibitor cocktail tablet (Roche) per 10 ml lysis-buffer).

Protein extract were separated by SDS-polyacrylamide gel electrophoresis (PAGE) was performed as described by and proteins were transferred to nitrocellulose membrane (Schleicher & Schuell, Den Bosch, The Netherlands) by western blotting. The membranes were blocked in 5% w/v non-fat dry milk in Tris-buffered saline-Tween 20 (TBST). The blots were incubated with a 1:1000 dilution of the indicated antibody in TBST with 3% BSA (Sigma) overnight at 4°C. Signal was detected using a 1:5000 dilution of horseradish peroxidase (HRP)-conjugated anti-rabbit antibodies and the enhanced chemiluminescence method (Amersham).

Acknowledgements

We gratefully acknowledge Jeroen den Hertog and Chris Joplin of the Hubrecht laboratory, for supplying probe-constructs, stimulating discussions and help with the cell tracing experiments. We thank Carl Philipp Heisenberg for discussions and probe-constructs, and Sophia von der Hardt from the Hammerschmidt lab., for providing us with the caged fluorescent dextran. In addition, we thank Tony Durston, Joost Woltering and Enrique Salas-Vidal for their contributions. This work was supported by a European Commission 6th Framework Program grant (contract LSHG-CT-2003-503496, ZF-MODELS).

References

1. Babb, S.G. and Marrs, J.A. (2004) E-cadherin regulates cell movements and tissue formation in early zebrafish embryos. Developmental Dynamics, 230, 263-277.
2. Bakkers, J., Kramer, C., Pothof, J., Quaedvlieg, N.E.M., Spaink, H.P., and Hammerschmidt, M. (2004) Has2 is required upstream of Rac1 to govern dorsal migration of lateral cells during zebrafish gastrulation. Development, 131, 525-537.
3. Brand, M., Heisenberg, C.P., Jiang, Y.J., Beuchle, D., Lun, K., Furutani-Seiki, M., Granato, M., Haffter, P., Hammerschmidt, M., Kane, D.A., Kelsh, R.N., Mullins, M.C., Odenthal, J., van Eeden, F.J., and Nusslein-Volhard, C. (1996) Mutations in zebrafish genes affecting the formation of the boundary between midbrain and hindbrain. Development, 123, 179-190.
4. Corson, L.B., Yamanaka, Y., Lai, K.M.V., and Rossant, J. (2003) Spatial and temporal patterns of ERK signaling during mouse embryogenesis. Development, 130, 4527-4537.
5. D'Amico, L.A. and Cooper, M.S. (2001) Morphogenetic domains in the yolk syncytial layer of axiating zebrafish embryos. Developmental Dynamics, 222, 611-624.
6. Daggett, D.F., Boyd, C.A., Gautier, P., Bryson-Richardson, R.J., Thisse, C., Thisse, B., Amacher, S.L., and Currie, P.D. (2004) Developmentally Restricted Actin-Regulatory Molecules Control Morphogenetic Cell Movements in the Zebrafish Gastrula. Current Biology, 14, 1632-1638.
7. Delfini, M.C., Dubrulle, J., Malapert, P., Chal, J., and Pourquie, O. (2005) Control of the segmentation process by graded MAPK/ERK activation in the chick embryo. PNAS, 102, 11343-11348.
8. Draper, B.W., Stock, D.W., and Kimmel, C.B. (2003) Zebrafish fgf24 functions with fgf8 to promote posterior mesodermal development. Development, 130, 4639-4654.
9. Furthauer, M., Lin, W., Ang, S.L., Thisse, B., and Thisse, C. (2002) Sef is a feedback-induced antagonist of Ras/MAPK-mediated FGF signalling. Nat Cell Biol, 4, 170-174.
10. Furthauer, M., Van Celst, J., Thisse, C., and Thisse, B. (2004) Fgf signalling controls the dorsoventral patterning of the zebrafish embryo. Development, 131, 2853-2864.
11. Gabay, L., Seger, R., and Shilo, B.Z. (1997) MAP kinase in situ activation atlas during Drosophila embryogenesis. Development, 124, 3535-3541.
12. Pagès G., Guérin G., Grall D., BoninoF., Smith A., Anjuere F., Auberger P. and Pouysségur J. (1999) Defective Thymocyte Maturation in p44 MAP Kinase (Erk1) Knockout Mice. Science, 286, 1374-1377.
13. Glickman, N.S., Kimmel, C.B., Jones, M.A., and Adams, R.J. (2003) Shaping the zebrafish notochord. Development, 130, 873-887.
14. Gotoh, Y., Masuyama, N., Suzuki, A., Ueno, N., and Nishida, E. (1995) Involvement of the Map Kinase Cascade in Xenopus Mesoderm Induction. Embo Journal, 14, 2491-2498.
15. Griffin, K., Patient, R., and Holder, N. (1995) Analysis of FGF function in normal and no tail zebrafish embryos reveals separate mechanisms for formation of the trunk and the tail. Development, 121, 2983-2994.

16. Griffin, K.J.P. and Kimelman, D. (2003) Interplay between FGF, one-eyed pinhead, and T-box transcription factors during zebrafish posterior development. Developmental Biology, 264, 456-466.
17. Grotegut, S., von Schweinitz, D., Christofori, G., and Lehembre, F. (2006) Hepatocyte growth factor induces cell scattering through MAPK/Egr-1-mediated upregulation of Snail. EMBO Journal, 25, 3534-3545.
18. Gryzik, T. and Muller, H.A.J. (2004) FGF8-like1 and FGF8-like2 encode putative ligands of the FGF receptor Htl for mesoderm migration and are required in the Drosophila gastrula. Current Biology, 14, 659-667.
19. Johnson, G.L., Dohlman, H.G., and Graves, L.M. (2005) MAPK kinase kinases (MKKKs) as a target class for small-molecule inhibition to modulate signaling networks and gene expression. Current Opinion in Chemical Biology, 9, 325-331.
20. Johnson, G.L. and Lapadat, R. (2002) Mitogen-Activated Protein Kinase Pathways Mediated by ERK, JNK, and p38 Protein Kinases. Science, 298, 1911-1912.
21. Jopling, C. and den Hertog, J. (2005) Fyn/Yes and non-canonical Wnt signalling converge on RhoA in vertebrate gastrulation cell movements. EMBO Reports, 6, 426-431.
22. Kane, D.A., Hammerschmidt, M., Mullins, M.C., Maischein, H.M., Brand, M., van Eeden, F.J., Furutani-Seiki, M., Granato, M., Haffter, P., Heisenberg, C.P., Jiang, Y.J., Kelsh, R.N., Odenthal, J., Warga, R.M., and Nusslein-Volhard, C. (1996) The zebrafish epiboly mutants. Development, 123, 47-55.
23. Kane, D.A., McFarland, K.N., and Warga, R.M. (2005) Mutations in half baked/E-cadherin block cell behaviors that are necessary for teleost epiboly. Development, 132, 1105-1116.
24. Kato, T., Ohtani-kaneko, R., Ono, K., Okado, N., and Shiga, T. (2005) Developmental regulation of activated ERK expression in the spinal cord and dorsal root ganglion of the chick embryo9. Neuroscience Research, 52, 11-19.
25. Kolch, W. (2005) Coordinating ERK/MAPK signalling through scaffolds and inhibitors. Nat Rev Mol Cell Biol, 6, 827-837.
26. Kozlowski, D.J., Murakami, T., Ho, R.K., and Weinberg, E.S. (1997) Regional cell movement and tissue patterning in the zebrafish embryo revealed by fate mapping with caged fluorescein. Biochemistry and Cell Biology-Biochimie et Biologie Cellulaire, 75, 551-562.
27. Krens, S.F.G., He, S., Spaink, H.P., and Snaar-Jagalska,B.E. (2006) Characterization and expression patterns of the MAPK family in zebrafish. Gene Expression Patterns, 6, 1019-1026.
28. LaBonne, C., Burke, B., and Whitman, M. (1995) Role of MAP kinase in mesoderm induction and axial patterning during Xenopus development. Development, 121, 1475-1486.
29. Lloyd, A. (2006) Distinct functions for ERKs? Journal of Biology, 5, 13.
30. Mathieu, J., Griffin, K., Herbomel, P., Dickmeis, T., Strahle, U., Kimelman, D., Rosa, F.M., and Peyrieras, N. (2004) Nodal and Fgf pathways interact through a positive regulatory loop and synergize to maintain mesodermal cell populations. Development, 131, 629-641.

31. Mazzucchelli, C., Vantaggiato, C., Ciamei, A., Fasano, S., Pakhotin, P., Krezel, W., Welzl, H., Wolfer, D.P., Pages, G., and Valverde, O. (2002) Knockout of ERK1 MAP Kinase Enhances Synaptic Plasticity in the Striatum and Facilitates Striatal-Mediated Learning and Memory. Neuron, 34, 807-820.
32. Medici, D., Hay, E.D., and Goodenough, D.A. (2006) Cooperation between snail and LEF-1 transcription factors is essential for TGF-beta 1-induced epithelial-mesenchymal transition. Molecular Biology of the Cell, 17, 1871-1879.
33. Montero, J.A. and Heisenberg, C.P. (2004) Gastrulation dynamics: cells move into focus. Trends in Cell Biology, 14, 620-627.
34. Myers, D.C., Sepich, D.S., and Solnica-Krezel, L. (2002) Convergence and extension in vertebrate gastrulae: cell movements according to or in search of identity? Trends in Genetics, 18, 447-455.
35. Ornitz, D. and Itoh, N. (2001) Fibroblast growth factors. Genome Biology, 2, reviews3005.1-3005.
36. Poulain, M., Furthauer, M., Thisse, B., Thisse, C., and Lepage, T. (2006) Zebrafish endoderm formation is regulated by combinatorial Nodal, FGF and BMP signalling. Development, 133, 2189-2200.
37. Pozios, K.C., Ding, J., Degger, B., Upton, Z., and Duan, C. (2001) IGFs stimulate zebrafish cell proliferation by activating MAP kinase and PI3-kinase-signaling pathways. Am J Physiol Regul Integr Comp Physiol, 280, R1230-R1239.
38. Raible, F. and Brand, M. (2001) Tight transcriptional control of the ETS domain factors Erm and Pea3 by Fgf signaling during early zebrafish development. Mechanisms of Development, 107, 105-117.
39. Saba-El-Leil, M.K., Vella, F.D.J., Vernay, B., Voisin, L., Chen, L., Labrecque, N., Ang, S.L., and Meloche, S. (2003) An essential function of the mitogen-activated protein kinase Erk2 in mouse trophoblast development. EMBO Reports, 4, 964-968.
40. Sawada, A., Shinya, M., Jiang, Y.J., Kawakami, A., Kuroiwa, A., and Takeda, H. (2001) Fgf/MAPK signalling is a crucial positional cue in somite boundary formation. Development, 128, 4873-4880.
41. Schier A.F., and Talbot. W. S. (2005) Molecular genetics of axis formation in zebrafish. Annu Rev Genet. 39, 561-613.
42. Sepich, D.S., Myers, D.C., Short, R., Topczewski, J., Marlow, F., and Solnica-Krezel, L. (2000) Role of the zebrafish trilobite locus in gastrulation movements of convergence and extension1. Genesis, 27, 159-173.
43. Shimizu, T., Yabe, T., Muraoka, O., Yonemura, S., Aramaki, S., Hatta, K., Bae, Y.K., Nojima, H., and Hibi, M. (2005) E-cadherin is required for gastrulation cell movements in zebrafish. Mechanisms of Development, 122, 747-763.
44. Solnica-Krezel, L. and Driever, W. (1994) Microtubule arrays of the zebrafish yolk cell: organization and function during epiboly. Development, 120, 2443-2455.
45. Solnica-Krezel, L. (2006) Gastrulation in zebrafish -- all just about adhesion? Current Opinion in Genetics & Development, 16, 433-441.

46. Stathopoulos, A., Tam, B., Ronshaugen, M., Frasch, M., and Levine, M. (2004) pyramus and thisbe: FGF genes that pattern the mesoderm of Drosophila embryos. Genes and Development, 18, 687-699.
47. Sun, X., Meyers, E.N., Lewandoski, M., and Martin, G.R. (1999) Targeted disruption of Fgf8 causes failure of cell migration in the gastrulating mouse embryo. Genes and Development, 13, 1834-1846.
48. Thisse, C., Thisse, B., Schilling, T.F., and Postlethwait, J.H. (1993) Structure of the zebrafish snail1 gene and its expression in wild-type, spadetail and no tail mutant embryos. Development, 119, 1203-1215.
49. Tsang, M., Friesel, R., Kudoh, T., and Dawid, I.B. (2002) Identification of Sef, a novel modulator of FGF signalling. Nat Cell Biol, 4, 165-169.
50. Tsang, M., Maegawa, S., Kiang, A., Habas, R., Weinberg, E., and Dawid, I.B. (2004) A role for MKP3 in axial patterning of the zebrafish embryo. Development, 131, 2769-2779.
51. Umbhauer, M., Marshall, C.J., Mason, C.S., Old, R.W., and Smith, J.C. (1995) Mesoderm Induction in Xenopus Caused by Activation of Map Kinase. Nature, 376, 58-62.
52. Uzgare, A.R., Uzman, J.A., El Hodiri, H.M., and Sater, A.K. (1998) Mitogen-activated protein kinase and neural specification in Xenopus. PNAS, 95, 14833-14838.
53. Vantaggiato, C., Formentini, I., Bondanza, A., Bonini, C., Naldini, L., and Brambilla, R. (2006) ERK1 and ERK2 mitogen-activated protein kinases affect Ras-dependent cell signaling differentially. Journal of Biology 5[5], 14.1-14.15.
54. Wilson, R., Vogelsang, E., and Leptin, M. (2005) FGF signalling and the mechanism of mesoderm spreading in Drosophila embryos. Development, 132, 491-501.
55. Yang, X., Dormann, D., Munsterberg, A.E., and Weijer, C.J. (2002) Cell Movement Patterns during Gastrulation in the Chick Are Controlled by Positive and Negative Chemotaxis Mediated by FGF4 and FGF8. Developmental Cell, 3, 425-437.
56. Yao, Y., Li, W., Wu, J., Germann,U.A., Su,M.S.S., Kuida,K., and Boucher,D.M. (2003). Extracellular signal-regulated kinase 2 is necessary for mesoderm differentiation. PNAS, 100, 12759-12764.

Supplementary data

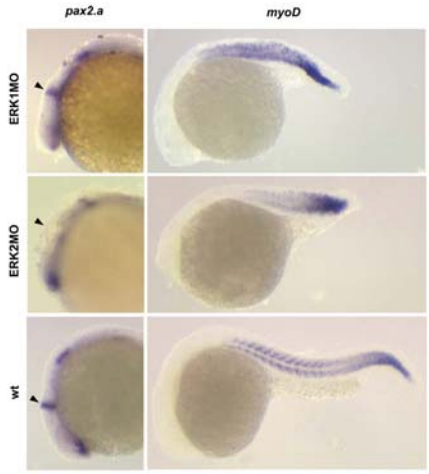

Figure S1. In situ hybridization with *pax2.1* or *myod* on ERK1MO or ERK2MO injected embryos compared to wild type embryos at 24hpf. Surviving embryos after knockdown of ERK1 or ERK2 show disturbed somite formation. Knockdown of ERK2 affects MHB formation.

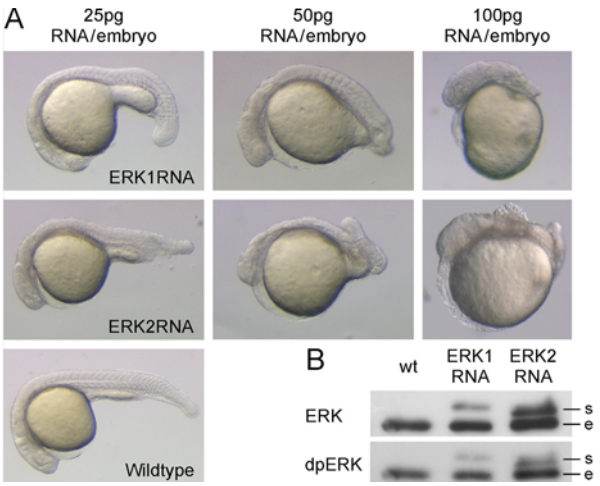

Figure S2. Over-expression of *erk1* and *erk2* led to concentration-dependent phenotypes. (A) Embryos were injected with 25, 50 or 100pg *erk1* RNA or *erk2* RNA per embryo and developmental phenotypes were recorded at 24hpf. (B) Western blot analysis was performed with global ERK and dpERK antibody on protein samples of 100pg RNA injected embryos in shield stage. The proteins derived from synthetic mRNAs (s) are slightly larger than the endogenous proteins (e) due to the introduction of a small linker, and can therefore be distinguished by size.

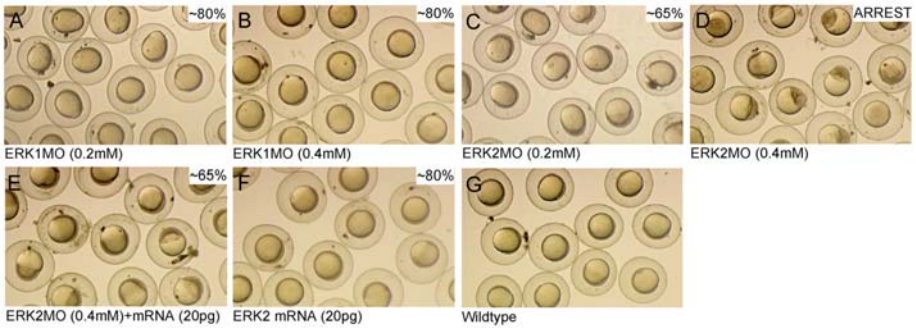

Figure S3. Specific functions of ERK1 and ERK2 revealed by concentration dependent knock-down during early embryogenesis. Embryos were injected with 0.2 mM (1.7 ng) and 0.4 mM (3.4 ng) ERK1MO (A,B) or ERK2MO (C,D) respectively. Rescue was performed by co-injection of 3.4ng ERK2MO with 20pg *erk2* mRNA (E) and compared to phenotypes of 20 pg *erk2* mRNA injected (F) and wild type embryos at 8hpf (H).